

Analysis and simulation of dynamic performance for DFIG-based wind farm connected to a distribution system

Author

Ghazanfar Shahgholian^{a*}

^a Smart Microgrid Research Center, Najafabad Branch, Islamic Azad University, Najafabad, Iran

Article history:

Received : 2 March 2017

Accepted : 8 April 2018

Keywords: DFIG; Wind Farm; Dynamic Performance.

ABSTRACT

Local renewable resources such as wind and solar are often available in remote locations. Wind farms consist of many individual wind turbines which are connected to the electric power transmission network. A wind farm can use the wind resources from a certain area efficiently. Double-fed induction generator (DFIG) is a generating principle widely used in wind turbine (WT). DFIG are able to generate active and reactive powers in an independent way. The objective of this paper is to study the improvement in dynamic performance conurbation from wind farms. Simulation studies were carried out in a two-machine power system. Different operating scenarios have been considered. Finally, some simulations are shown to support the improvement in dynamic performance of the DFIG based WT.

1. Introduction

There are a wide range of sources of power in power systems such as falling water (hydroelectric power), steam heated using fossil fuel or nuclear energy and wind (wind power) [1,2]. Wind is an internal source of energy. Wind energy is clean, renewable and is an inexhaustible source of energy. Wind power involves the conversion of energy from the wind into other types of useful energy. The main advantage of wind energy is that its exploitation doesn't pollute the environment or disrupt natural processes, unlike many other energy sources [3]. Large groups of wind turbines are called wind farms. A large wind farm can contain hundreds of wind turbines spread out over hundreds of miles.

They are becoming an increasingly important source of intermittent renewable energy and are used by many countries as part of a strategy to reduce their reliance on fossil fuels [4].

The doubly-fed induction generator (DFIG) system is a popular system in which the power electronic interface controls the rotor currents to achieve the variable speed necessary for maximum energy capture in variable winds [5,6]. Many works have been done and published on the application of DFIG based wind turbine in power system [7,8]. The influence of control performance of PSS auxiliary loops for specific DFIG control scheme is demonstrated in [9]. The relative capabilities of PSS controllers based on rotor speed, stator power and network frequency, and when the DFIG turbine is subjected to aerodynamic torque variations, were investigated via simulation studies. A control

* Corresponding author: Ghazanfar Shahgholian
Smart Microgrid Research Center, Najafabad Branch,
Islamic Azad University, Najafabad, Iran
Email: shahgholian@iaun.ac.ir

law based on the passivity theory for wind farms equipped with DFIG operating in a network with a complex load for damping frequency oscillations after a network disturbance is presented in [10]. Multi-objective optimal controller design of a DFIG wind turbine system using differential evolution is presented in [11], where the steady-state stability and dynamic performance at different operating conditions are implemented to optimize the controller parameters of both the rotor and grid-side converters. The effect of replacing one existing synchronous generator with a power system stabilizer by a DFIG on the local mode and the mode shapes of the critical inter-area modes are analyzed in [12]. A quantitative assessment of transient stability for power systems integrated with DFIG wind farms is proposed in [13] by evaluating the transient energy margin (TEM) through the formulation of the transient energy function (TEF) for power system. A feedback linearization controller based on the detailed model of the doubly fed induction generator based wind turbine to maximize energy conversion is demonstrated in [14], where the stability of the remained internal dynamics is analyzed via Lyapunov stability method. A method to control the output active power of a DFIG-based wind farm with the aim of improving the transient stability of a power system is proposed in [15], where the variation of the frequency of the DFIG terminal bus is used to modulate the torque reference and thus

the output power of the DFIG in the post-disturbance condition. A switching angle controller and an automatic generation controller for the DFIG to control the frequency of DFIG-based wind power penetrated power systems is proposed in [16].

In this paper, the dynamic performance of a wind farm connected to a distribution system is described. Matlab Simulink software package is used for the simulations. Simulation results are presented under various operating conditions. Simulation results show that good transient stability and steady state responses can be obtained in the system.

2. Doubly-Fed Induction Generator

The generators used for wind turbine applications can be classified into four main concepts as shown in Fig. 1. Doubly-fed electric machines are electric motors or electric generators where both the field magnet windings and armature windings are separately connected to equipment outside the machine [17, 18]. By feeding adjustable frequency ac power to the field windings, the magnetic field can be made to rotate, allowing variation in motor or generator speed. This is useful, for instance, for generators used in wind turbines [19,20]. The overall configuration of a DFIG based wind turbine is shown schematically in Fig. 2. It consists of a wind turbine, a gearbox, a DFIG and back-to-back converters [21,22].

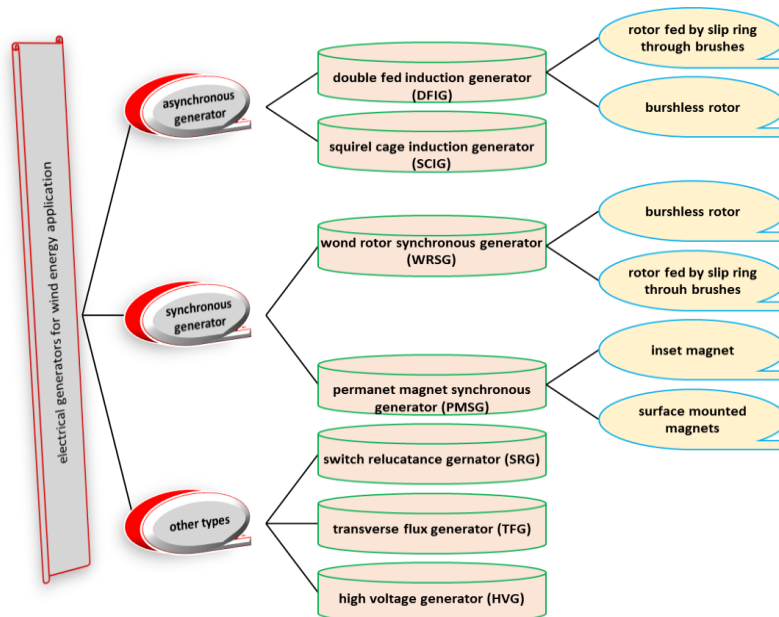


Fig. 1. Different types of generator used in wind energy conversion system

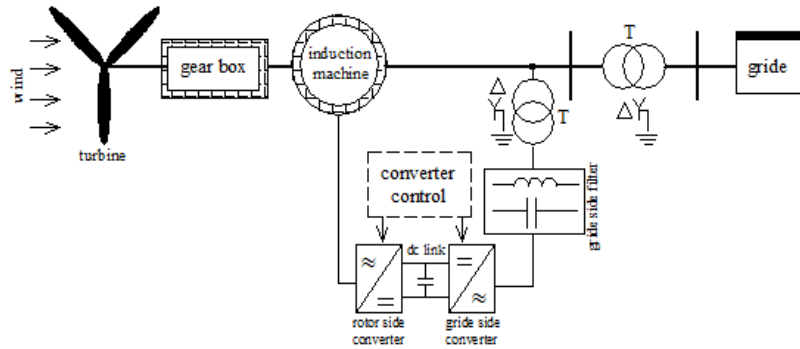


Fig. 2. Basic configuration of a DFIG for a wind turbine application

Using the motor convention, the relation between the voltages on the machine windings and the currents, the DFIG was represented in terms of a synchronous reference dq frame by the following equations [23,24]:

$$u_{sd} = R_S i_{sd} + \frac{d\lambda_{sd}}{dt} - \omega_s \lambda_{sq} \quad (1)$$

$$u_{sq} = R_S i_{sq} + \frac{d\lambda_{sq}}{dt} + \omega_s \lambda_{sd} \quad (2)$$

$$u_{rd} = R_R i_{rd} + \frac{d\lambda_{rd}}{dt} - (\omega_s - \omega_r) \lambda_{sq} \quad (3)$$

$$u_{rq} = R_R i_{rq} + \frac{d\lambda_{rq}}{dt} + (\omega_s - \omega_r) \lambda_{sd} \quad (4)$$

where u_{ds} and u_{qs} are the direct and quadrature components of the stator voltage, u_{rd} and u_{rq} are the direct and quadrature components of the rotor voltage, i_{ds} and i_{qs} are the direct and quadrature components of the stator currents, i_{rd} and i_{rq} are the direct and quadrature components of the rotor current. ω_r is the generator angular frequency and ω_s is the synchronous angular frequency. The stator flux

components λ_{sd} and λ_{sq} and the rotor flux components λ_{rd} and λ_{rq} are given by [25,26]:

$$\begin{cases} \lambda_{sd} = L_S i_{sd} + L_M i_{rd} \\ \lambda_{sq} = L_S i_{sq} + L_M i_{rq} \end{cases} \quad (5)$$

$$\begin{cases} \lambda_{rd} = L_R i_{rd} + L_M i_{sd} \\ \lambda_{rq} = L_R i_{rq} + L_M i_{sq} \end{cases} \quad (6)$$

where L_S and L_R are the stator and rotor windings self-inductance, L_M is the mutual inductance between the stator and the rotor [27]. The DFIG equivalent circuit is shown in Fig. 3. This model is able to represent rotor and stator transients correctly [28,29].

3. Wind turbine Model

A wind turbine can be considered as a highly nonlinear system. According to the resultant energy type, a mechanical part (wind turbine with blades, shaft and gearbox) and an electrical part (generator, converters and other electrical control units) constitute two parts of a wind generation system. A wind turbine is a complex system. A model of the wind energy conversion

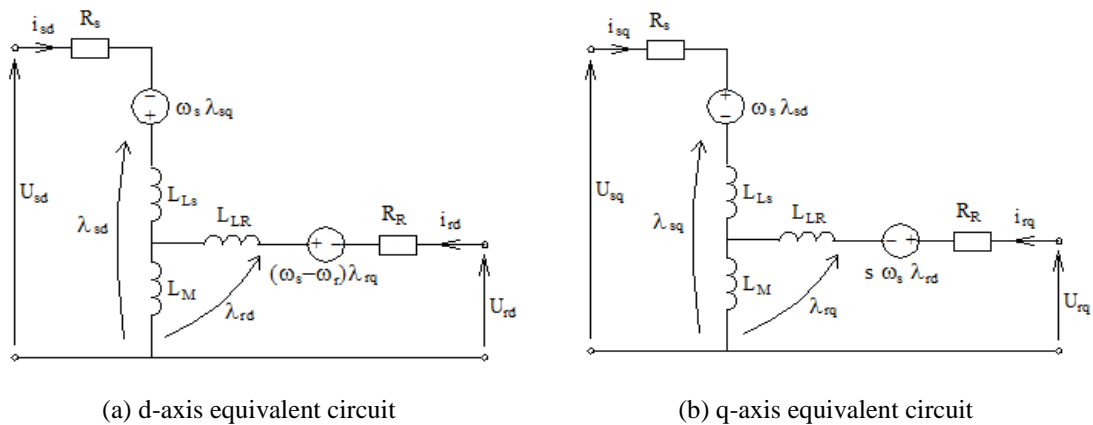


Fig. 3. Equivalent circuit of a DFIG

system can be represented using several interconnected subsystems as shown in Fig. 4, where F_t is structural forces, ω_r is shaft speed, T_t is hub torque, T_g is reaction torque, ω_g is generator rotor speed and P_o is power demand.

A wind turbine is characterized by the curves of the dimensionless power coefficient (C_p) which is a nonlinear function of both tip speed ratio (λ) and blade pitch angle (β) [30]. Power coefficient known as performance coefficient

calculates the fraction of power a wind turbine can extract from the wind. Fig. 5 depicts the graph of the power coefficient versus pitch angle and tip speed. For each wind turbine, a rated wind speed is specified. In below-rated wind speed, the controller priority is to maximize the energy capture. In above-rated wind speed, the controller tries to shed the excess power in the wind. A typical power curve is shown in Fig. 6.

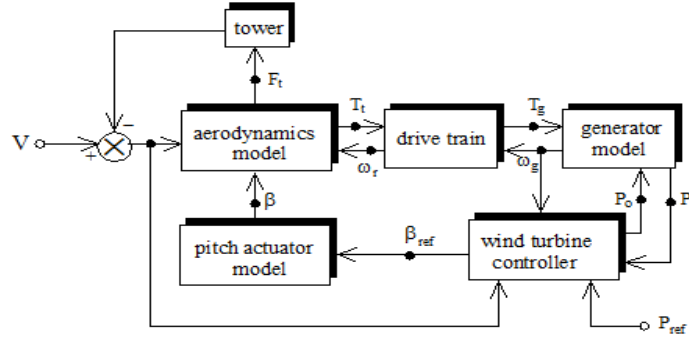


Fig. 4. Block diagram of a wind energy conversion system

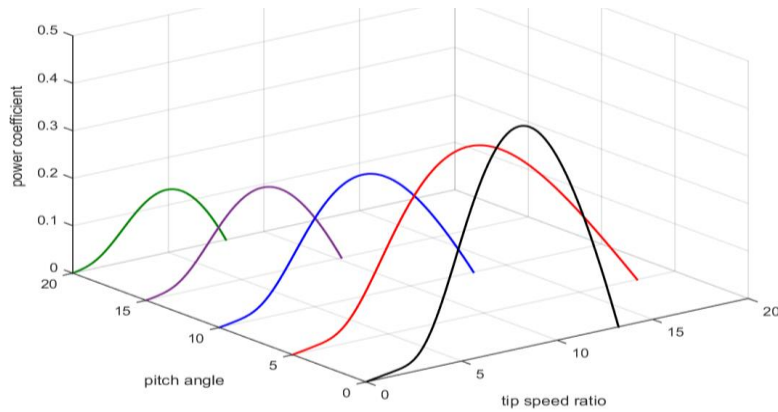


Fig. 5. A typical power coefficient characteristic for pitch angle between 0° and 20°

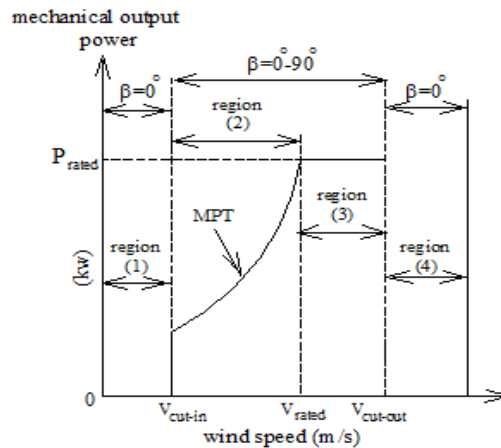


Fig. 6. Ideal power curve of a wind turbine operation zone

4. Power System Description

A wind farm is a group of wind turbines in the same location used to produce electricity. In a wind farm, individual turbines are interconnected with a medium voltage power collection system and communications network.

Single-line diagram of the wind farm connected to a distribution system is shown in Fig. 7. In this system, a 9 MW wind farm is connected to a 25 KV (U_w) distribution system that exports power to a 120 KV (U_G) grid via a transmission line (lines L_1 and L_2), 25 KV feeder (bus 1). Wind turbines use a DFIG consisting of a wound rotor induction generator and a PWM converter. The 9 MW wind farm is an aggregated model of 6 wind turbine units, where each unit has a power rating of 1.5 MW. The stator winding is connected directly to the 60 Hz network while the rotor is fed at variable frequency through the converter. A 2.3 KV, 2

MVA plant consisting of a motor load and a 200 KW resistive load is connected on the same feeder at bus 2. A 500 KW load is also connected on the bus 4 of the wind farm. The motor load is 1.68 MW induction motor at 0.93 PF.

5. Simulation Results

Block diagram of the wind farm connected to the distribution system and block diagram of the 2 MVA plant with its protection system are presented in Figs. 8 and 9, respectively. Both the motor load and the wind turbine have a protection system monitoring voltage, current and machine speed.

Simulations are performed for four cases: wind speed change, voltage sag, load change and three phase fault. In this section, the system is observed during 40 s.

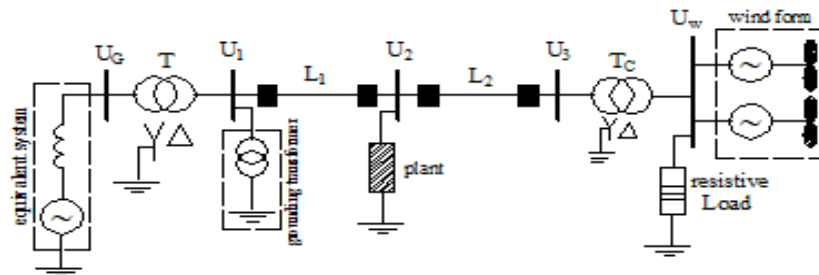


Fig. 7. Single-line diagram of the wind farm connected to a distribution system

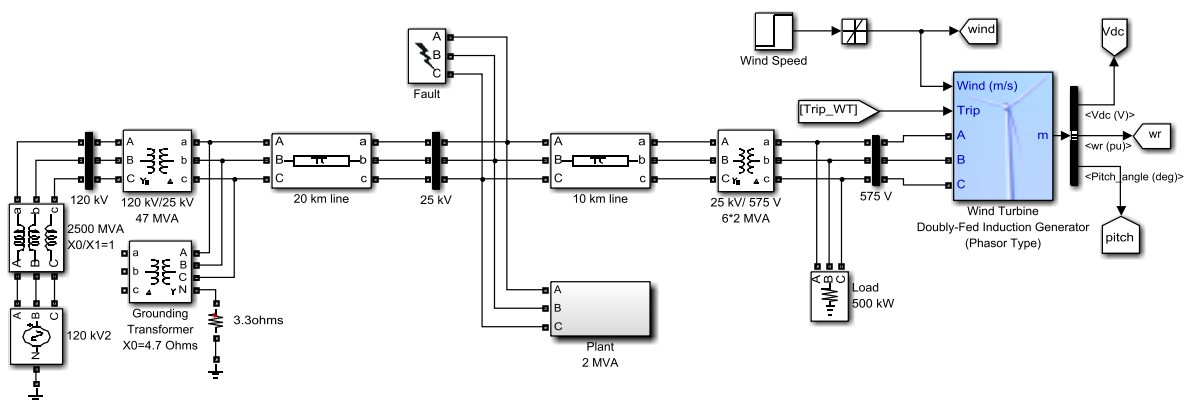


Fig. 8. Schematic diagram of the simulated system in Simulink MATLAB

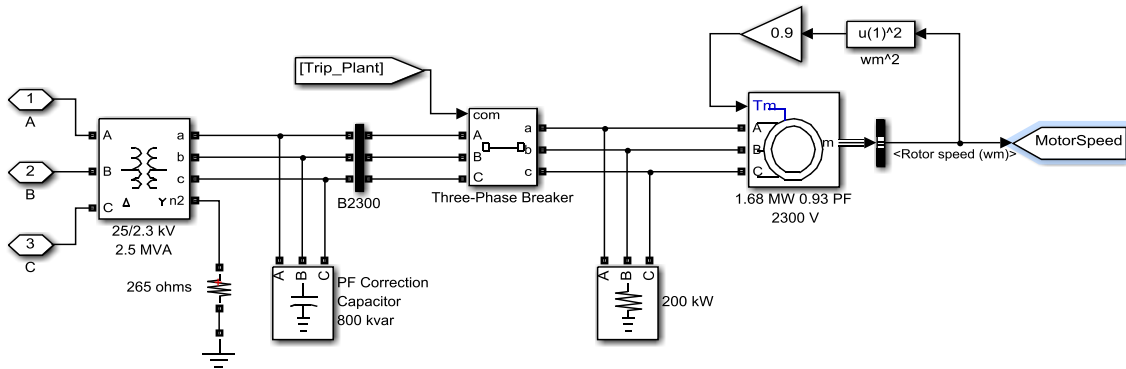


Fig. 9. Block diagram of the 2 MVA plant with its protection system in Simulink MATLAB

5.1. Wind speed change

Initially, wind speed is set at 8 m/s, and that at $t=5$ s, wind speed increases suddenly at 14 m/s as shown in Fig. 10. The generated active power and reactive power are shown in Fig. 11. At $t = 5$ s, the generated active power starts increasing smoothly to reach its rated value of 9 MW in approximately 15 s. The reactive power is controlled to maintain a 1 pu voltage. At nominal power, the wind turbine generated -0.68 MVAR to control voltage at 1 pu.

Initially, the pitch angle of the turbine blades is 0° . The pitch angle is shown in Fig. 12. It is increased from 0° to 0.76° in order to limit the mechanical power. The turbine speed is shown in Fig. 13. It increased from 0.8 to 1.21 pu. The turbine mechanical power as function of turbine speed is displayed for wind

speeds ranging from 5 to 16.2 m/s. The changes of power at bus plant under change in wind turbine is shown in Fig. 14.

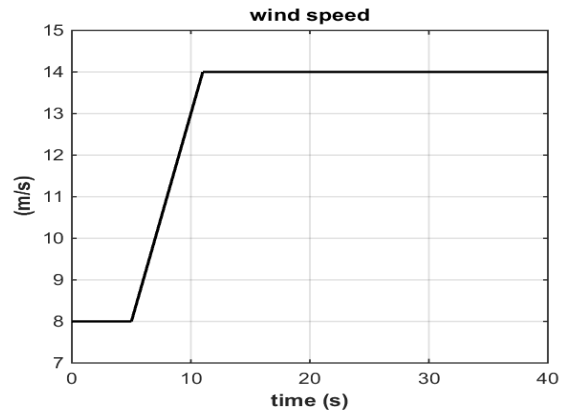


Fig. 10. Change in wind speed

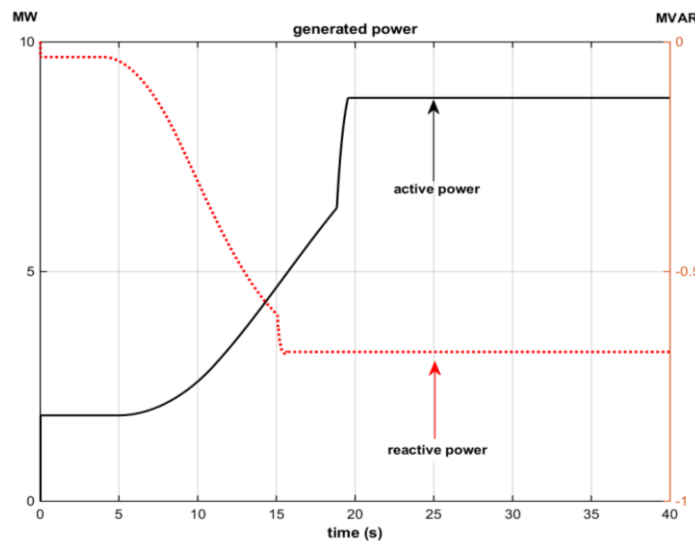


Fig. 11. Generated power by wind farm under change in wind turbine

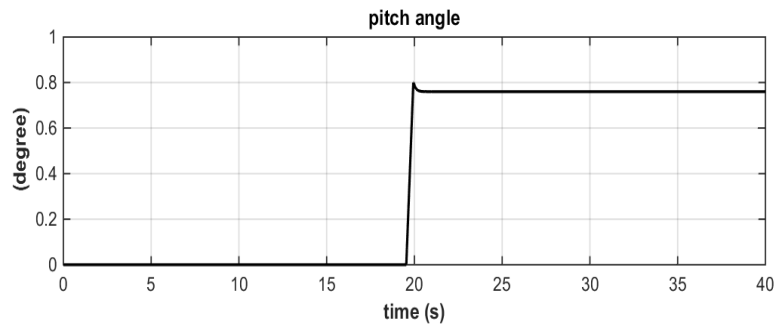


Fig. 12. Pitch angel under change in wind turbine

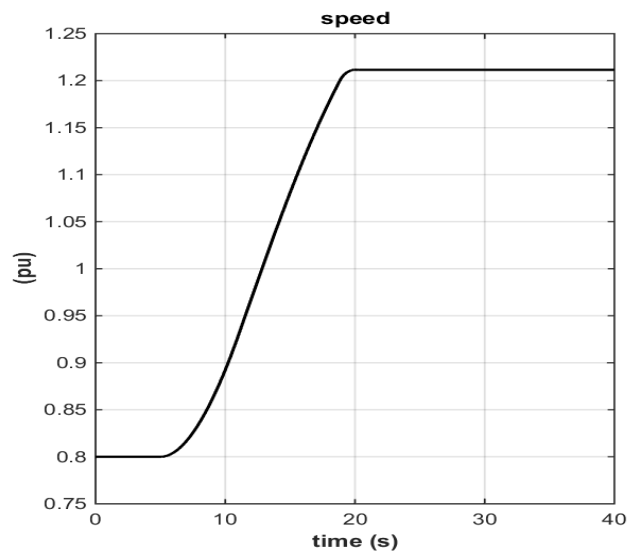


Fig. 13. Turbine speed under change in wind turbine

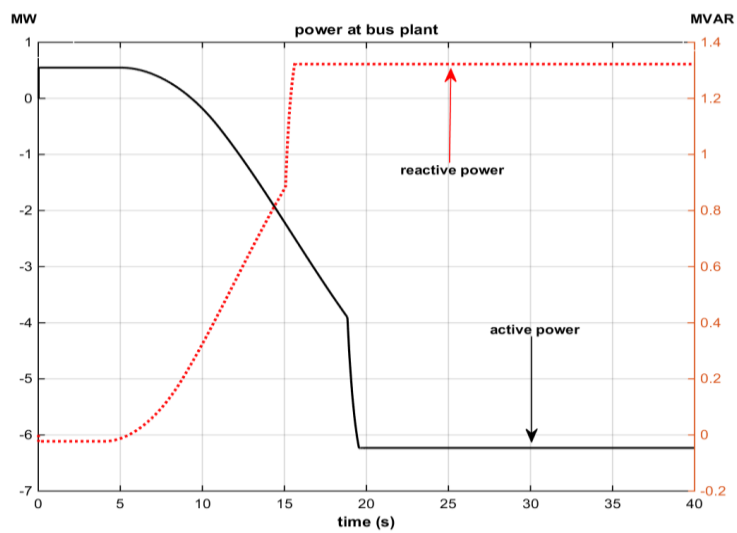


Fig. 14. Power at bus plant under change in wind turbine

5.2. Single to ground fault at wind turbine terminal

In this scenario, a single phase to ground fault occurs on the transmission line. The pitch angle is zero. The wind speed is 8 m/s. A 9 cycle single-phase to ground is applied on phase A at U2 bus. It occurs at the fifth sec. The generated active power and reactive power are shown in Fig. 15 for 4.5 to 5.5 s. The positive sequences voltage and current at wind turbine terminal are shown in Fig. 16. The positive sequence voltage drops to 0.8 pu during the fault, which is above the under voltage protection threshold of 0.75 pu for a

$t > 0.1$ s. The turbine speed increases as shown in Fig. 17.

5.3. Three-phase to ground fault

In this scenario, a three-phase to ground fault occurs on the transmission line. The wind speed is 8 m/s. A 9 cycle three-phase to ground is applied at U2 bus. It occurs at the fifth sec.

Voltage and current at wind turbine terminal under three-phase to ground fault is shown in Fig. 18. Pitch angle and turbine speed under three-phase to ground fault are shown in Figs. 19 and 20, respectively.

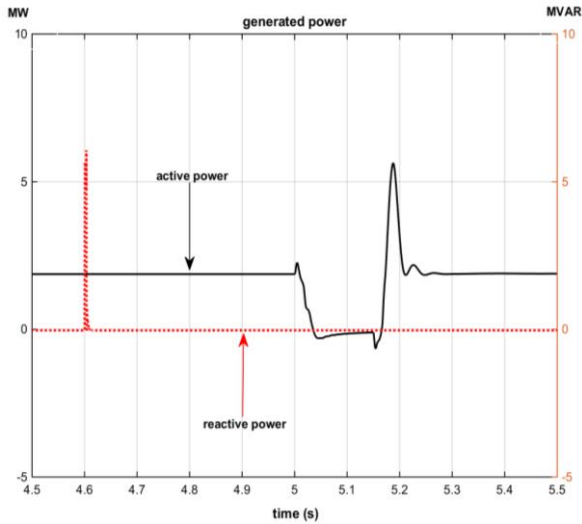


Fig. 15. Generated power by wind farm under single to ground fault

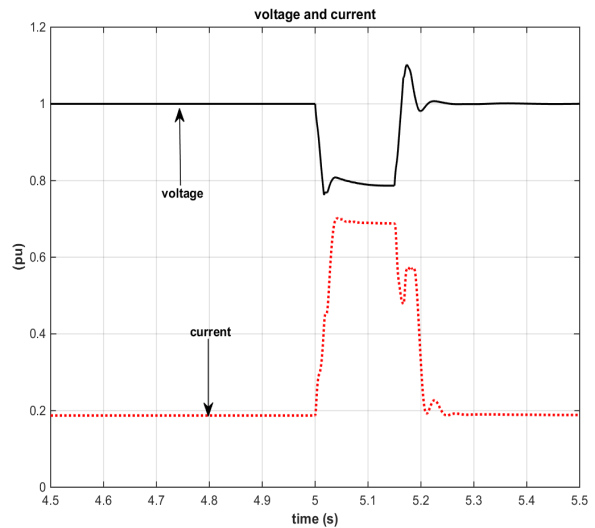


Fig. 16. Voltage and current at wind turbine terminal under single to ground fault

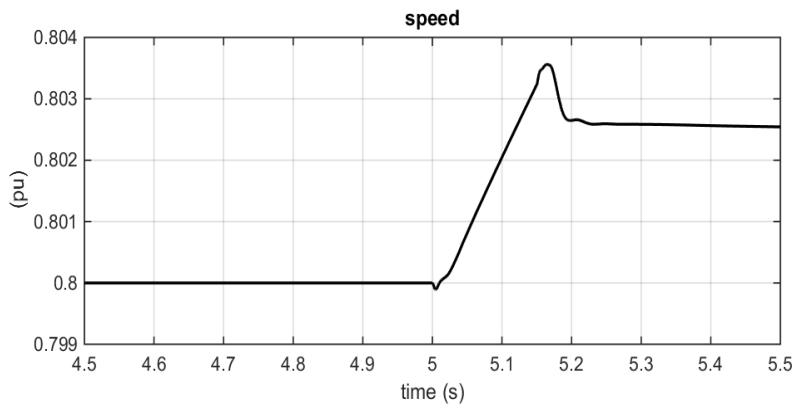


Fig. 17. Turbine speed under single to ground fault

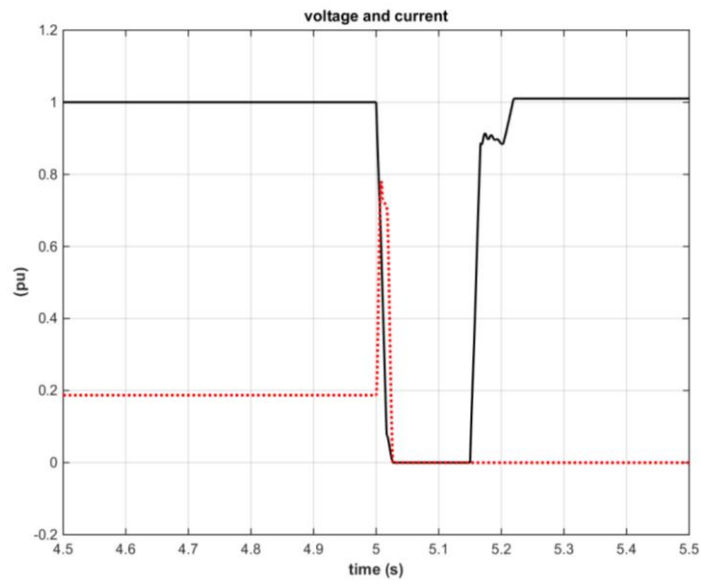


Fig. 18. Voltage and current at wind turbine terminal under three-phase to ground fault

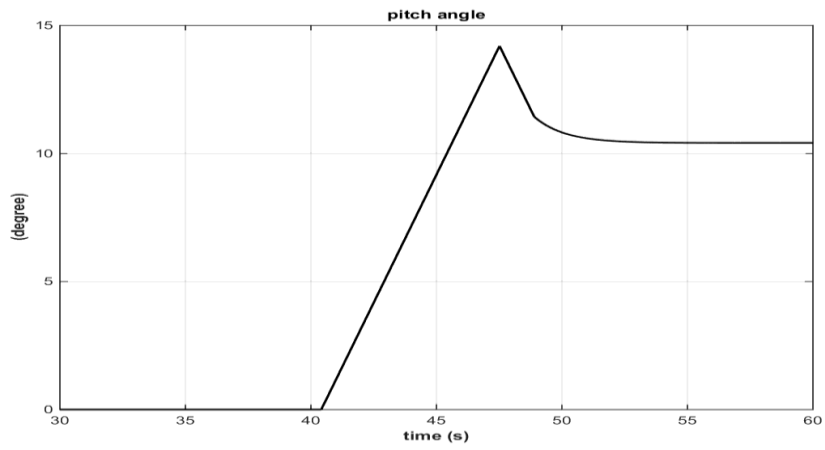


Fig. 19. Pitch angle under three-phase to ground fault

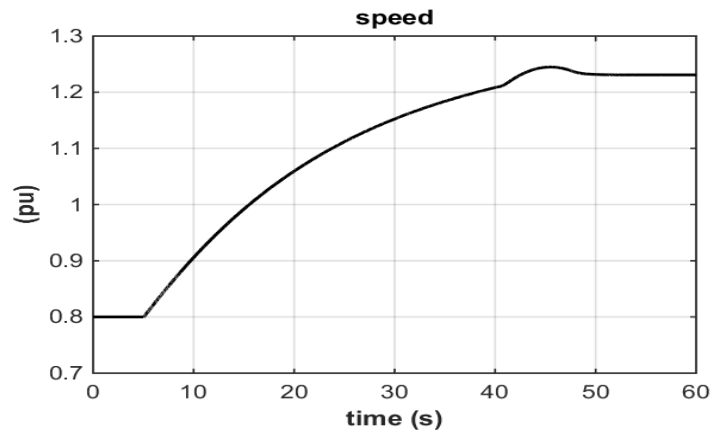


Fig. 20. Turbine speed under three-phase to ground fault

5.4. Three-phase to ground fault

In this section, the impact of a voltage sag resulting from a remote fault on the generator bus will be displayed. The wind speed is constant at 8 m/s. A 0.15 pu voltage drop lasting 0.5 s, is shown in Fig. 21, in the voltage source (U_G). It occurs at the fifth sec. The generated active power by wind farm is shown in Fig. 22. It produces 1.87 MW. The motor

speed is shown in Fig. 23, which decreases gradually. As shown in Fig. 24, the plant voltage during the voltage sag is 0.93 pu and above the 0.9 pu protection threshold. This is because the voltage support is provided by the 5 MVAR reactive power generated by the wind-turbines as shown in Fig. 25. Active power at plant bus is shown in Fig. 26.

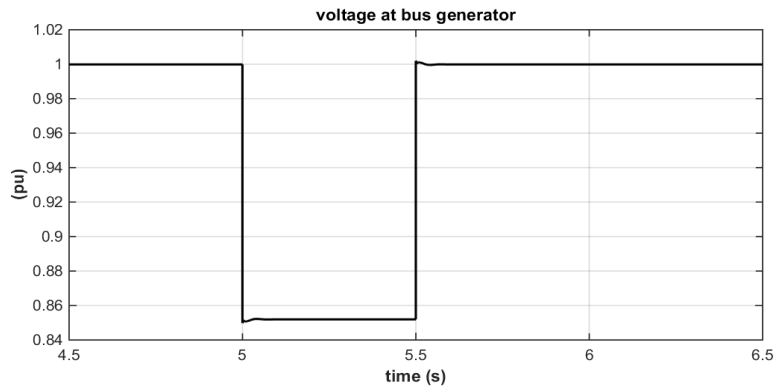


Fig. 21. Voltage source under a voltage sag

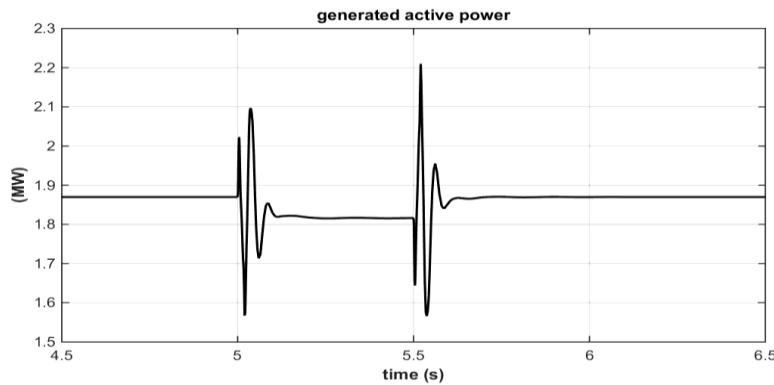


Fig. 22. Generated active power by wind farm during the voltage sag

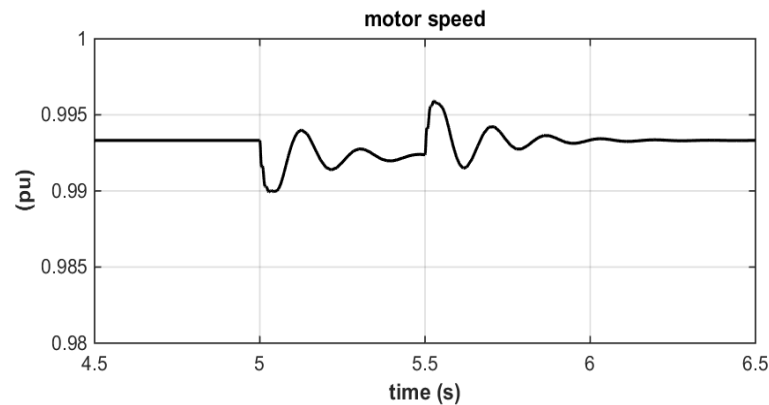


Fig. 23. Motor speed during the voltage sag

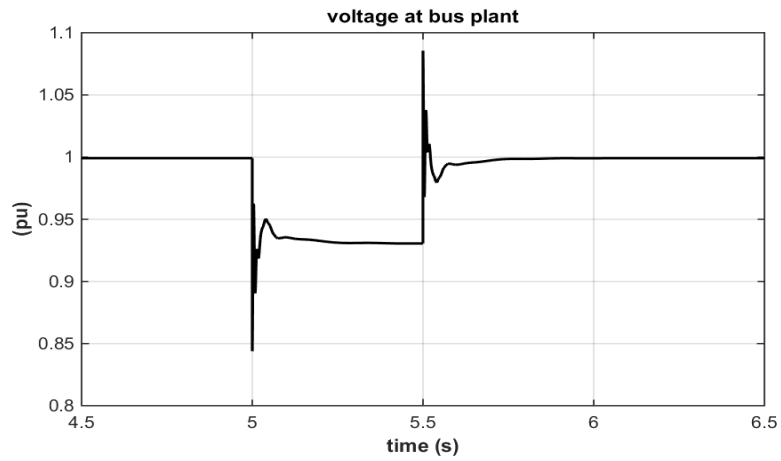


Fig. 24. Plant voltage during the voltage sag

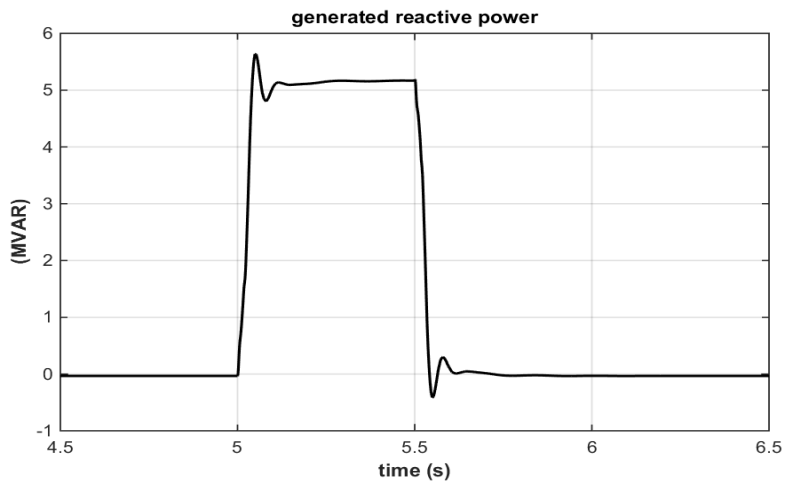


Fig. 25. Generated reactive power by wind farm during the voltage sag

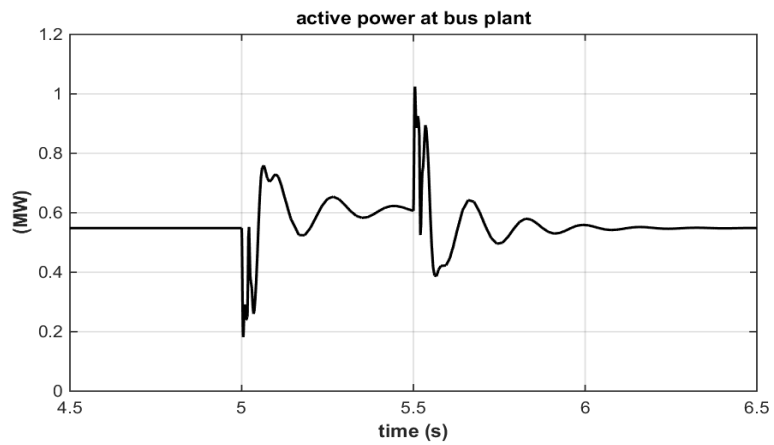


Fig. 26. Active power at bus plant during the voltage sag

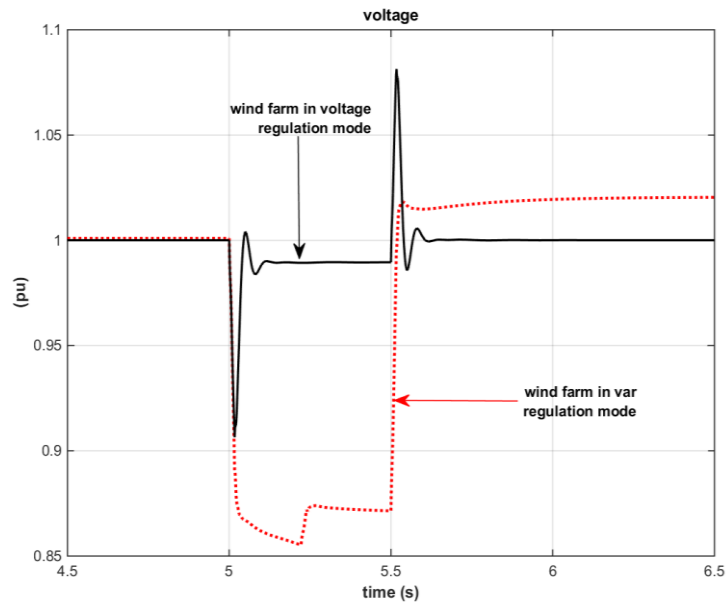


Fig. 27. Plant voltage during the voltage sag

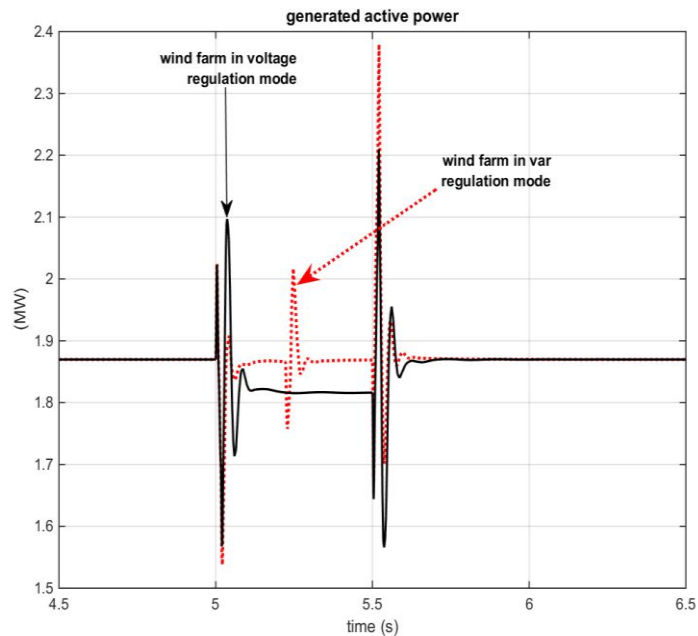


Fig. 28. Active power generated by wind turbine during the voltage sag

Figs. 27 and 28 show the plant voltage and generated active power by wind farm turbine on the two modes of operation of the wind turbine: voltage regulation and VAR regulation.

6. Conclusion

Wind energy is considered as one of the most important green energies and has been

developed and applied worldwide. The modeling of a DFIG-based wind farm connected to a distribution system has been described to study the steady-state and dynamic performance. The simulation results are validated under various scenarios. Simulation results are presented to demonstrate the effectiveness of the wind farm to improve the power system transient stability.

References

- [1] Bhatt P., Ghoshal S.P., Roy R., Coordinated Control of TCPS and SMES for Frequency Regulation of Interconnected Restructured Power Systems with Dynamic Participation from DFIG Based Wind Farm, *Renewable Energy* (2012) 40(1):40-50.
- [2] Shahgholian G., Power System Stabilizer Application for Load Frequency Control in Hydro-Electric Power Plant, *Engineering Mathematics* (2017) 2(1):21-30.
- [3] Shahgholian G., Khani K., Moazzami M., Frequency Control in Autanamous Microgrid in the Presence of DFIG Based Wind Turbine, *Journal of Intelligent Procedures in Electrical Technology* (2015) 6(23): 3-12.
- [4] Mozafarpour-Khoshrodi S.H., Shahgholian G., Improvement of Perturb and Observe Method for Maximum Power Point Tracking in Wind Energy Conversion System Using Fuzzy Controller, *Energy Equipment and Systems* (2016) 4(2):111-122.
- [5] Lopez J., Gubia E., Sanchis P., Roboam X., Wind Turbines Based on Doubly Fed Induction Generator under Asymmetrical Voltage Dips, *The IEEE Transactions on Energy Conversion* (2008) 23(1):321-330.
- [6] Liu H., Xie X., Zhang C., Li Y., Liu H., Hu Y., Quantitative SSR Analysis of Series-Compensated DFIG-Based Wind Farms Using Aggregated RLC Circuit Model, *The IEEE Transactions on Power Systems* (2017) 32(1): 474-483.
- [7] Javaheri-Fard H., Najafi H.R., Eliasi H., Active and Reactive Power Control Via Currents of a Rotor's d and q Components with Nonlinear Predictive Control Strategy in a Doubly Fed Induction Generator Based on Wind Power System, *Energy Equipment and Systems* (2015) 3(2) 143-157.
- [8] Song Y., Wang X., Blaabjerg F., High-frequency Resonance Damping of DFIG-Based Wind Power System under Weak Network, *The IEEE Transactions on Power Electronics* (2017) 32(3): 1927-1940.
- [9] Hughes F.M., Anaya-Lara O., Ramtharan G., Jenkins N., Strbac G., Influence of Tower Shadow and Wind Turbulence on the Performance of Power System Stabilizers for DFIG-Based Wind Farms, *The IEEE Transactions on Energy Conversion* (2008) 23(2):519-528.
- [10] Fernández R.D., Mantz R.J., Battaiotto P.E., Wind Farm Control for Stabilisation of Electrical Networks Based on Passivity, *International Journal of Control* (2010)83(1):105-114.
- [11] Yang L., Yang G.Y., Xu Z., Dong Z.Y., Wong K.P., Ma X., Optimal Controller Design of a Doubly-Fed Induction Generator Wind Turbine System for Small Signal Stability Enhancement, *IET Generation, Transmission and Distribution* (2010) 4(5): 579–597 579.
- [12] Chaudhuri N.R., Chaudhuri B., Considerations Toward Coordinated Control of DFIG-Based Wind Farms, *The IEEE Transactions on Power Delivery* (2013) 28(3): 1263-1270.
- [13] Chowdhury M.A., Shen W., Hosseinzadeh N., Pota H.R., Transient Stability of Power System Integrated with Doubly Fed Induction Generator Wind Farms, *IET Renewable Power Generation* (2015) 9(2): 184–194.
- [14] Yang B., Jiang L., Wang L., Yao W., Wu Q.H., Nonlinear Maximum Power Point Tracking Control and Modal Analysis of DFIG Based Wind Turbine, *International Journal of Electrical Power and Energy Systems* (2016) 74: 429–436.
- [15] Mitra A., Chatterjee D., Active Power Control of DFIG-Based Wind Farm for Improvement of Transient Stability of Power Systems, *The IEEE Transactions on Power Systems* (2016) 31(1): 82-93.
- [16] Liu Y., Jiang L., Wu Q.H., X. Zhou, Frequency Control of DFIG-Based Wind Power Penetrated Power Systems Using Switching Angle Controller and AGC, *The IEEE Transactions on Power Systems* (2017) 32(2): 1553-1567.
- [17] Fooladgar M., Rok-Rok E., Fani B., Shahgholian G., Evaluation of the Trajectory Sensitivity Analysis of the DFIG Control Parameters in Response to Changes in Wind Speed and the Line Impedance Connection to the Grid DFIG, *Journal of Intelligent Procedures in Electrical Technology* (2015) 5(20): 37-54.
- [18] Hong M., Xin H., Liu W., Xu Q., Zheng T., Gang D., Critical Short Circuit Ratio Analysis of the DFIG Wind Farm with Vector Power Control and Synchronized Control, *Journal of Electrical Engineering and Technology* (2016) 11(2): 320-328, 2016.
- [19] Mehta B., Bhatt P., Pandya V., Small Signal Stability Enhancement of DFIG Based Wind Power System Using

- Optimized Controllers Parameters, *International Journal of Electrical Power and Energy Systems* (2015) 70: 70–82.
- [20] Shahgholian G., Khani K., Moazzami M., The Impact of DFIG Based Wind Turbines in Power System Load Frequency Control with Hydro Turbine, Dam and Hydroelectric Powerplant (2015) 1(3): 38-51.
- [21] Chena Q., Lib Y., Seemc J.E., Dual-loop Self-Optimizing Robust Control of Wind Power Generation with Doubly-Fed Induction Generator, *ISA Transactions* (2015) 58: 409–420.
- [22] Mohammadpour H.A., Santi E., Modeling and Control of Gate-Controlled Series Capacitor Interfaced with a DFIG-Based Wind Farm, *The IEEE Transactions on Industrial Electronics* (2015) 62 (2): 1022-1033.
- [23] Koa H.S., Yoonb G.G., Kyunga N.H., Hongc W.P., Modeling and Control of DFIG-Based Variable-Speed Wind-Turbine, *Electric Power Systems Research* (2008) 78(11):1841–1849.
- [24] Geng H., Liu C., Yang G., LVRT Capability of DFIG-Based WECS under Asymmetrical Grid Fault Condition, *The IEEE Transactions on Industrial Electronics* (2013) 60(6): 2495-2509.
- [25] Ghennam T., Aliouane K., Akel F., Francois B., Berkouk E.M., Advanced Control System of DFIG Based Wind Generators for Reactive Power Production and Integration in a Wind Farm Dispatching, *Energy Conversion and Management* (2015) 105: 240–250.
- [26] Shahgholian G., Izadpanahi N., Improving the Performance of Wind Turbine Equipped with DFIG Using STATCOM Based on Input-Output Feedback Linearization Controller, *Energy Equipment and Systems* (2016) 4(1): 65-79.
- [27] Song Z., Shi T., Xia C., Chen W., A Novel Adaptive Control Scheme for Dynamic Performance Improvement of DFIG-Based Wind Turbines, *Energy* (2012) 38(1): 104–117.
- [28] Fan L., Zhu C., Miao Z., Hu M., Modal Analysis of a DFIG-Based Wind Farm Interfaced with a Series Comp-ensated Network, *The IEEE Transactions on Energy Conve-rs-i-on* (2011) 26(4):1010-1020.
- [29] Fan L., Kavasseri R., Miao Z.L., Zhu C., Modeling of DFIG-Based Wind Farms for SSR Analysis, *The IEEE Transactions on Power Delivery* (2010) 25(4): 2073-2082.
- [30] Muyeen S.M., Takahashi R., Murata T., Tamura J., A Variable Speed Wind Turbine Control Strategy to Meet Wind Farm Grid Code Requirements, *The IEEE Transactions on Power Systems* (2010) 25(1):331-340.